Pergamon

0042-6989(95)00114-X

Vision Res. Vol. 35, No. 22, pp. 3083–3091, 1995

0042-6989/95 $9.50 + 0.00

Photoreceptor Spectral Sensitivities: Common Shape in the Long-wavelength Region

T. D. LAMB*

Received 16 January 1995; in revised form 24 March 1995

Previous measurements of mammalian photoreceptor spectral sensitivity have been analysed, with particular attention to the long-wavelength region. The measurements selected for study come from rod and cone systems, and from human, monkey, bovine and squirrel sources. For the spectra from photoreceptor electrophysiology and from psychophysical sensitivity, the frequency scaling applied by Mansfield (1985, *The visual system*, pp. 89–106. New York: Alan Liss) provides a common shape over a range of at least 7 $\log_{10}$ units of sensitivity, from low frequencies (long wavelengths) to frequencies beyond the peak. The same curve is applicable to the absorbance spectrum of bovine rhodopsin, although the absorbance can only be measured down to about 2 $\log_{10}$ units below the peak. At the longest wavelengths the results exhibit a common limiting slope of 70 $\log_e$ units (or 30.4 $\log_{10}$ units) per unit of normalized frequency. A simple equation is presented as a generic description for the α-band of mammalian photoreceptor spectral sensitivity curves, and it seem likely that the equation may be equally applicable to retinal$_1$-based pigments in other species. Despite the lack of a theoretical basis, the equation has the correct asymptotic behaviour at long wavelengths, and it provides an accurate description of the peak. It also accounts accurately for the experimentally observed "yellowing" of long-wavelength lights that occurs beyond 700 nm.

Photoreceptor Visual pigment Spectral sensitivity Wavelength

INTRODUCTION

The spectral sensitivity of human vision was first measured through psychophysical experiments in the early part of this century (for references see Goodeve, 1936; Crawford, 1949). More recently, the spectral sensitivities of the rod and cone photopigments have been studied by a variety of methods: by spectrophotometry using extracted pigments, by psychophysical experiments in which the different cone mechanisms are differentially "adapted out", by retinal densitometry, by microspectrophotometry on intact photoreceptor outer segments and by electrophysiological recordings from individual photoreceptors. In this paper, results from selected measurements of spectral sensitivity (made both recently, and as long as 60 yr ago) are drawn together, in an attempt to determine a common spectral shape for mammalian photopigments.

Spectral templates

For a number of rhodopsins displaying a range of peak wavelengths (λ_{max}), Dartnall (1953) reported that the absorbance spectra had a closely similar shape when plotted on a frequency scale (frequency $\nu = c/\lambda$). He extracted a "nomogram" (or template) to describe their common form, which he claimed could simply be slid along the frequency axis. Subsequently, Ebrey and Honig (1977) studied photopigments exhibiting a wider range of maxima than had been examined by Dartnall, with the λ_{max} of their retinal$_1$-based pigments ranging from 427 to 575 nm. They found that the spectral bandwidth ($\nu_{1/2}$) of the curves, rather than being constant as proposed by Dartnall, actually varied continuously, roughly in proportion to the peak frequency (ν_{max}). As an approximate means of accounting for this, they invoked three separate templates in different regions of the spectrum. An elegant alternative, providing a return to a single spectral shape, was reported by Mansfield (1985) who found that an invariant template could be obtained for primate cone absorbance spectra simply by plotting the results against normalized frequency, ν/ν_{max}.

One of the main purposes of this paper is to examine further the applicability of the Mansfield normalization to photoreceptor spectral sensitivity curves. Special emphasis is placed on the long-wavelength region where both psychophysical and electrophysiological experiments have enabled the sensitivity to be followed down to extremely low levels.

The spectral sensitivity of individual mammalian photoreceptor cells has been examined in monkey rods (Baylor, Nunn & Schnapf, 1984), in monkey cones (Baylor, Nunn & Schnapf, 1987), in squirrel cones (Kraft,

*Physiological Laboratory, University of Cambridge, Downing Street, Cambridge CB2 3EG, England.

1988), in human cones (Schnapf, Kraft & Baylor, 1987) and in human rods (Kraft, Schneeweis & Schnapf, 1993). For the red, green and blue cones from monkey, Baylor *et al.* (1987) found that the Mansfield scaling applied accurately. They presented a sixth-order polynomial expression which provided a good description of the spectral template over the wavelength region plotted; however at slightly longer wavelengths that expression diverges seriously from the known behaviour. In addition, they reported that their cone spectrum was somewhat broader than the spectrum obtained previously for monkey rods by Baylor *et al.* (1984). For squirrel cones Kraft (1988) found a shape generally similar to, but apparently different from, that found for monkey cones by Baylor *et al.* (1987). Subsequently Kraft *et al.* (1993) reported that the spectral shape for human rods differed from that for monkey rods, and appeared to be the same as that for monkey cones. The results from those studies form the basis of the photoreceptor electrophysiological spectra presented here.

From human psychophysical experiments, Stockman, MacLeod and Johnston (1993) found that the shapes of the cone spectral sensitivities were closely similar when plotted on a normalized frequency basis, but they concluded that a slight difference in shape existed between the red and green cone spectra.

Recently Stavenga, Smits and Hoenders (1993) used the Mansfield normalization approach to obtain a new estimate of the common spectral template. They concentrated on fitting the absorbance spectrum that had been obtained by Partridge and de Grip (1991) for bovine rhodopsin. The present study differs from that approach by concentrating initially on the sensitivity in the long-wavelength region, obtained from electrophysiological and psychophysical measurements. This provides a means firstly of examining the applicability of the Mansfield transformation, and secondly (in conjunction with the absorbance measurements) of estimating the shape of the common spectral sensitivity curve.

In comparing spectral sensitivity curves, it is important to ensure that the same sensitivity parameter is being measured. In the early psychophysical work analysed here, the sensitivity curves were based on light measurements in units of energy rather than of photons. As first pointed out by Dartnall and Goodeve (1937), a proper comparison with absorbance curves necessitates conversion to photon units of intensity, which may be done simply by scaling the energy-based sensitivities in inverse proportion to wavelength. Thus, in conformity with most other recent work, all sensitivities in this paper are determined on a photon basis. The details of this conversion, and of other corrections, are presented in the Methods.

Behaviour at very long wavelengths

The sensitivity of the human *photopic* visual system in the far red was investigated by Goodeve (1936), out to a wavelength of 900 nm. His measurements showed that, when plotted against frequency, the $\log_{10}$ photopic sensitivity declined as a straight line with a slope of 17.02 μm; i.e. $\log_{10}$ sensitivity (in energy units) = constant + 17,020/λ, with λ in nm. Upon conversion to photon units this slope equals 17.4 μm (see Methods). Comparable results were subsequently reported by Wald (1945), Pinegin (1945) and Griffin, Hubbard and Wald (1947), the latter two reports extending the observations to 950 and 1000 nm respectively. For the human *scotopic* system, extensive measurements of sensitivity were made by Crawford (1949) for 50 observers, over the range 380–780 nm. Although not explicitly stated by Crawford, his tabulated results show that in the long-wavelength region the $\log_{10}$ sensitivity (converted to photon units) declined as a straight line against frequency, with a slope of 15.3 μm.

A theoretical basis for the straight line relation between $\log_{10}$ sensitivity and frequency was proposed by Stiles (1948) on energy considerations. He postulated that a "low-energy" photon could be absorbed provided that the sum of the photon energy and the thermal energy of the rhodopsin molecule exceeded some fixed energy barrier. On the simplest assumptions this led to the prediction that sensitivity would be proportional to $\exp(-hc/kT\lambda)$, where h is Planck's constant, c is the velocity of light, k is Boltzmann's constant and T is absolute temperature. When plotted in $\log_e$ units against $1/\lambda$ this expression predicted a straight line with a slope of hc/kT; in $\log_{10}$ units this corresponds to a slope of $0.4343hc/kT$, equal to 20.2 μm at body temperature. In examining the experimental values reported in the literature, Stiles found that the measured slope for the scotopic system was 79%, and for the photopic system 87%, of his prediction.

A revised theory was formulated by Lewis (1955), who introduced multiple modes of vibration in the rhodopsin molecule. For scotopic vision he obtained a good fit to the experimental slope using seven vibrational modes, and for photopic vision using three or four. However that formulation has not received subsequent theoretical support, and neither it nor the earlier approach of Stiles can account for the decline in sensitivity at short wavelengths.

Brindley (1955) discovered that at very long wavelengths the colour of light appeared to revert from red towards orange. The subjective sensation of the deepest red colour was found to occur for illumination at 700 nm, and for longer wavelengths a match could be obtained with illumination of shorter wavelengths. Thus, for example, a light of 850 nm (when made sufficiently bright) matched the orange-red colour of illumination at 652 nm. Since the blue cones are essentially unresponsive at these wavelengths, Brindley interpreted the observations to indicate a change in the ratio of red cone to green cone sensitivity beyond 700 nm, and hence to show that in the long-wavelength region the slope of the log sensitivity profile was slightly smaller for the green cones than for the red cones. Much more recently, electrophysiological recordings of spectral sensitivity have been made from individual mammalian photoreceptor cells (cited above). The long-wavelength slopes obtained in these experiments have confirmed the values measured

long ago in psychophysical experiments on the scotopic and photopic systems.

The great advantage of measurements at very long wavelengths is that they enable the spectral sensitivity to be followed down to extremely low values. This approach is employed in the present paper to examine the similarity in shape of the spectral sensitivity curves from different mammalian species.

METHODS

The psychophysical sensitivity measurements were converted to spectral absorbances as follows.

Conversion from energy to photon units. Since the energy per photon is hc/λ, the psychophysical spectral sensitivity measurements expressed in energy units were converted to photon units by dividing by wavelength and then renormalizing to unit peak height. In the long-wavelength region, where the $\log_{10}$ sensitivity declines as a straight line against $1/\lambda$, the slope expressed in energy units can be converted to a slope in photon units by adding $0.4343\lambda_{slp}$, where λ_{slp} (in μm) is the wavelength at which the slope was determined.

Multiple receptor mechanisms. To convert photopic sensitivity measurements to values relative to the peak of the red cone mechanism, it is necessary to allow for the fact that photopic sensitivity is mediated by more than one class of cone. There is, however, some uncertainty in assigning a precise value for the relative contribution of the red and green cones to photopic sensitivity. The ratio of red cone to green cone input was estimated as 2:1 by Walraven (1974), although slightly lower values are obtained by more recent work. R. W. Rodieck (personal communication) has estimated a ratio of 1.83, based on calculations of Stockman *et al.* (1993, p. 2515). However, this ratio is considerably higher than the ratio of numbers of red cones to green cones in monkey retina, which is approximately 1:1 (Mollon & Bowmaker, 1992). Accordingly, it seems reasonable to adopt a ratio intermediate between these values, of about 1.5. Denoting the input weightings as r and g, and adding the weighted spectral curves of the red and green cones, the peak photopic sensitivity is found to be approx. $0.96(r+g)/r$ times greater than the peak sensitivity of the red cones, giving a factor of 1.6. Hence the photopic sensitivity measurements of Goodeve (1936) and Griffin *et al.* (1947), which were plotted and tabulated only at wavelengths longer than 614 nm, but which were expressed relative to the peak sensitivity at 556 nm, have been scaled up by a factor of 1.6 (0.2 $\log_{10}$ units) here. This correction is however only approximate, firstly because in those early papers the experimental details of the normalization to peak photopic sensitivity were not described explicitly, and secondly because the relative input of the red and green cones to photopic sensitivity remains an estimate.

Self-screening. Self-screening has been corrected for, assuming a peak optical density, D, for the photopigment of 0.4 $\log_{10}$ units in the rods and 0.27 $\log_{10}$ units in the cones, with axial incidence of light; the cone value is taken from Baylor *et al.* (1987), although Stockman *et al.* (1993) have suggested a larger value. Thus, the normalized sensitivity, S, was replaced by $\log_{10}[1 - S(1 - 10^{-D})]/(-D)$.

Pre-retinal filtering. The spectral shape of the pre-retinal filtering (contributed predominantly by the lens) has been tabulated by Wyszecki and Stiles (1982), and adjusted slightly by Stockman *et al.* (1993, Table 7). In the present paper, that optical density was approximated by the expression $1.1\exp((400-\lambda)/15) + 0.11\exp((500-\lambda)/80)$, with λ in nm. The macula pigment is not relevant, since scotopic results were obtained in the peripheral retina, while photopic results were obtained only at wavelengths longer than 556 nm

TABLE 1. Symbols, slopes and source of the results in Figs 1–3

Symbol	λ_{max} (nm)	Measurement	Species	Method	Slope (μm) This paper	Slope (μm) Original paper	Source of data Reference	Source of data Table
■	561	Red cone sensitivity	Monkey	Φ	17.05	17.2	Baylor *et al.* (1987)	1
◆	533	Green cone sensitivity	Monkey	Φ	16.20	15.9	Baylor *et al.* (1987)	1
▲	431	Blue cone sensitivity	Monkey	Φ	13.10	12.7	Baylor *et al.* (1987)	1
○	523	Green cone sensitivity	Squirrel	Φ	15.90	(14.6)	Kraft (1988)	Fig. 6
▼	440	Blue cone sensitivity	Squirrel	Φ	13.38	(11.1)	Kraft (1988)	Fig. 6
●	496	Rod sensitivity	Monkey	Φ	15.08	15.0	Baylor *et al.* (1984)	1
•	496	Rod sensitivity	Human	Φ	15.08	14.7	Kraft *et al.* (1993)	1
★	498	Rod absorbance	Bovine	Abs	15.14	—	Partridge and de Grip (1991)	1
□	561	Photopic sensitivity	Human	Ψ	17.05	(17.4)	Goodeve (1936)	Fig. 1
□	561	Photopic sensitivity	Human	Ψ	17.05	(17.4)	Griffin *et al.* (1947)	5
○	496	Scotopic sensitivity	Human	Ψ	15.08	(15.3)	Crawford (1949)	4

The solid symbols were obtained in electrophysiological (Φ) experiments on single photoreceptors from monkey, squirrel or human retina. The ★ were obtained from absorbance measurements (Abs) on extracted bovine rhodopsin. The open symbols were obtained in psychophysical (Ψ) experiments on dark-adapted human observers; see Methods for the conversions applied to these psychophysical values. The second column (λ_{max}) gives the wavelength scaling employed in the present study to obtain a common shape. The two columns headed "Slope" give the limiting slope of $\log_{10}$ sensitivity at long wavelengths: the sixth column was obtained from the scaling required to fit equation (2) in the present study (see text). The seventh column was obtained from the original studies, either as the value given by the authors, or (in parentheses) by re-measurement from the original data. The final column gives the table in the cited reference from which the results have been taken, except for Goodeve (1936) and Kraft (1988) where the values were not tabulated and have instead been extracted from the figures indicated.

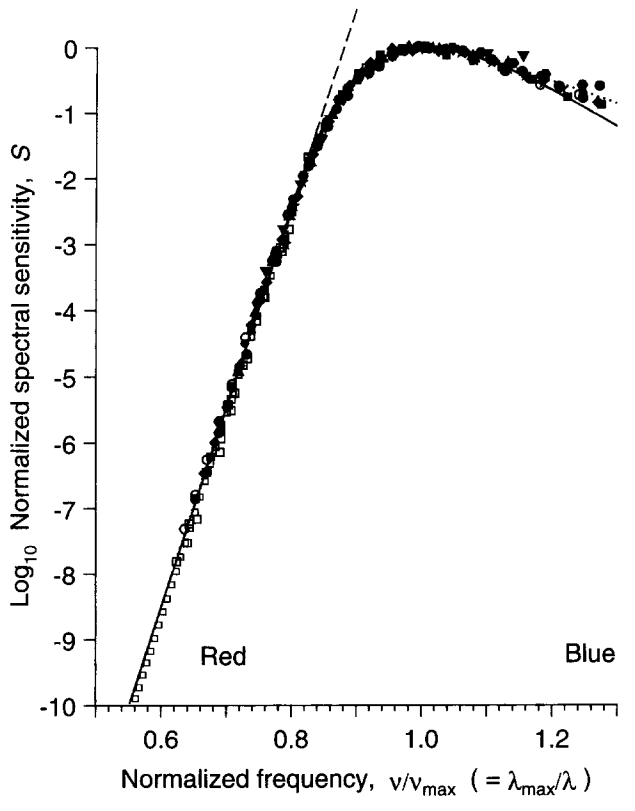

FIGURE 1. Normalized spectral sensitivities (in photon units) on a logarithmic scale, plotted as a function of normalized frequency. The symbols, identified in Table 1, have been taken from raw measurements of photoreceptor electrophysiology (monkey, squirrel and human) and of spectrophotometry (bovine rhodopsin), and by conversion from energy-based psychophysical sensitivity results (photopic and scotopic) as described in Methods. The dotted curve is equation (1) with $a = 72$, $b = 8$ and $n = 4$. The solid curve is equation (2) with $a = 70$, $b = 28.5$, $c = -14.1$, $A = 0.880$, $B = 0.924$, $C = 1.104$ and $D = 0.655$. The dashed straight line is the first term in equation (2); i.e. a slope of 70 $\log_e$ units (or 30.4 $\log_{10}$ units) per unit of normalized frequency.

where macular absorption is negligible (Wyszecki & Stiles, 1982).

Electrophysiological spectra. A minor correction has been made to the plotting of the electrophysiological results. In their Table 1, Baylor *et al.* (1987) assigned the sensitivities of both the red cones and the green cones as unity at 559 nm. Here, those tabulated values have been normalized to the respective cone peaks by decreasing all the green cone values by 0.02 $\log_{10}$ units and by increasing all the red cone values by 0.02 $\log_{10}$ units.

RESULTS

Normalized spectral sensitivity curves

The spectral sensitivities measured in the studies selected from the literature (see Table 1) are plotted in normalized form in Figs 1 and 2. All the plots are referenced to photon (rather than energy) units, and the conversions that have been applied to the psychophysical measurements are described in Methods. In Fig. 1 the sensitivity is plotted on a logarithmic scale, whereas in Fig. 2 it is plotted on a linear scale. In both figures the sensitivity has been normalized to its maximum value (as is conventional), and in addition the frequency scale has been normalized to the frequency of maximum sensitivity [i.e. $x = \nu/\nu_{max} = \lambda_{max}/\lambda$, as proposed by Mansfield (1985)]; this scale has been restricted to $\nu/\nu_{max} > 0.7$ in Fig. 2, as the points are indistinguishable from zero at lower frequencies. The same symbols are used in both figures, and are identified in Table 1. Table 1 also identifies the original papers from which the results were taken, and gives the wavelength scaling (λ_{max}) employed in the present study.

Perhaps the most striking result in Figs 1 and 2 is the close similarity in the shape of the spectral curves obtained from the different sources. Identically the same curves are plotted as the solid and dotted traces in the two figures, and the form of these curves is discussed in a subsequent section.

In the logarithmic plot of Fig. 1, the points at low frequencies (long wavelengths) in the different experiments are indistinguishable from each other over a range of at least 7 $\log_{10}$ units of sensitivity. Hence Fig. 1 extends Mansfield's finding of a common spectral shape a further 5 $\log_{10}$ units down in sensitivity than could be examined with his absorbance measurements. It also indicates that the common shape appears to be applicable to results obtained from single-cell electrophysiology, from spectrophotometry on extracted pigment (bovine rhodopsin) and from psychophysical sensitivity.

Another clear result of Fig. 1 is that in the long-wavelength region the decline of log sensitivity for all the points is well-fitted by a straight line. Previously it has been shown that in any given set of measurements the log sensitivity at long wavelengths declines as a straight line when plotted against frequency. The results of Fig. 1 extend those observations by showing that different pigments all exhibit the *same* slope when plotted against normalized frequency. This means that, when plotted on a raw scale of absolute (rather than normalized) frequency, the limiting slope of the log sensitivity will be directly proportional to the λ_{max} of the pigment. As we shall see below, this finding provides a good description for the "yellowing" of red light that Brindley (1955) observed at very long wavelengths.

In the linear plot of Fig. 2 the substantial degree of scatter in the filled symbols simply illustrates the finite accuracy of the electrophysiological technique, for recordings with a limited number of flash responses. This scatter does not appear to indicate any systematic deviation from a common shape, at least for frequencies up to the peak. Figure 2 also illustrates the high level of internal consistency in the absorbance measurements (★). These points show very low variability in a linear plot, but they cannot reliably be followed down below an absorbance level of about 1% because the magnitude of the error is approximately constant in absolute terms.

Limiting slope at long wavelengths

The magnitude of the limiting slope at long wavelengths, shown by the dashed line in Fig. 1, is 70 $\log_e$ units (or 30.4 $\log_{10}$ units) per unit of normalized frequency. Multiplying by the values of λ_{max} used in the

scaling, this common normalized slope converts to the absolute slopes given in column 6 of Table 1. For example, for monkey red cones (■) fitted with a λ_{max} of 561 nm, the curve corresponds to a $\log_{10}$ slope (against $1/\lambda$) of 30.4×561 nm $= 17.05$ μm. For comparison, the adjacent column in Table 1 gives the slopes obtained from the original papers, either by the authors or (where not given, or given in energy terms) by fitting a straight line to the results plotted in photon terms. The values in the two columns are generally in very good agreement. The largest discrepancy occurs for squirrel blue cones, where the sensitivity was only followed down about 3.5 $\log_{10}$ units so that the true asymptotic slope was probably not attained.

A template curve

It would be very valuable to obtain a simple template curve describing the common spectral shape; thus an expression is required for the normalized sensitivity $S(x)$ as a function of the normalized frequency, $x = \nu/\nu_{max}$ $(=\lambda_{max}/\lambda)$. Ideally, such a curve should be based on firm theoretical principles, but regrettably an adequate theory of light absorption by visual pigments does not appear to have been developed. In the absence of a comprehensive theory, it seemed that the logical starting point would be to describe the straight-line region at long wavelengths and then to try to obtain a simple description for the remainder of the spectral curve.

Curve 1. The simplest curve found to provide a reasonable description was

$$S(x) = \{A\exp(-ax/n) + B\exp(bx/n)\}^{-n}. \quad (1)$$

Plotted in log sensitivity co-ordinates, this equation has a limiting slope of $a\log_e$ units for small x, and $-b\log_e$ units for large x, and it changes slope between these limits over a width that depends on the exponent n. Two of the five constants in the expression are redundant because of the normalization; thus the peak occurs at $x = 1$, so we can write $dS/dx = 0$ and $S = 1$ at $x = 1$. This gives $A = b/(a + b)\exp(a/n)$ and $B = a/(a + b)\exp(-b/n)$; hence equation (1) involves only three parameters: a, b and n. It was found that an adequate fit to the results in the logarithmic plot of Fig. 1 could be obtained with $a = 72$, $b = 8$ and $n = 4$; this fit is plotted as the dotted curve in Figs 1 and 2. However, in the linear plot of Fig. 2 this equation appears to deviate significantly from the results (especially for the absorbance measurements, ★) on either side of the peak, i.e. near $x \approx 0.88$ and $x \approx 1.15$.

Curve 2. An alternative expression that was found to provide a better fit, but which employed more parameters, was the reciprocal of the sum of three exponential terms:

$$S(x) = \{\exp a(A-x) + \exp b(B-x) + \exp c(C-x) + D\}^{-1}. \quad (2)$$

Once again, two of the parameters in this equation are redundant, since the peak occurs at $x = 1$, with zero slope and unit amplitude; however the resulting interrelations between parameters are quite complicated and will not be given here. The solid curves in Figs 1 and 2 were obtained from equation (2), with the slopes of the three exponentials given by $a = 70$, $b = 28.5$ and $c = -14.1$ [note the sign reversal in the third term in equation (2)], and with the three position constants $A = 0.880$, $B = 0.924$ and $C = 1.104$, and with the final constant $D = 0.655$. Inspection of Figs 1 and 2 shows that with these parameters equation (2) provides a very good description of the common behaviour.

It needs to be emphasized that the above represents no more than an exercise in curve-fitting, and that neither equation (1) nor equation (2) has any known physical

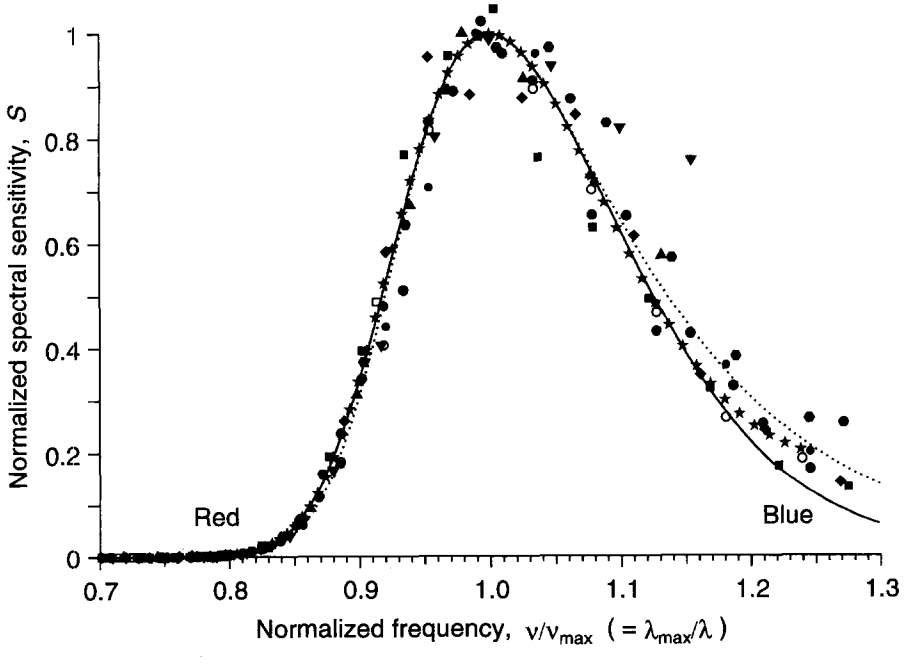

FIGURE 2. The same results as in Fig. 1, plotted on a linear ordinate scale, and with the abscissa restricted to $x > 0.7$. The symbols are identified in Table 1. The dotted and solid curves plot equations (1) and (2) respectively, as in Fig. 1.

significance, apart from the asymptotic slope at long wavelengths. Although both curves provide an acceptable fit in the double logarithmic co-ordinates of Fig. 1 (and indeed are hidden beneath the symbols for the most part), the additional requirement of fitting the results in the linear ordinate scale of Fig. 2 presents a demanding test. Finding an expression that provides both an adequate fit near the peak in Fig. 2, as well as the correct asymptotic slope in Fig. 1, proved to be difficult. An alternative way of expressing this is to say that the combination of sensitivity measurements (applicable out to the far red) with absorbance measurements (having high accuracy in the vicinity of the peak) provides a rigorous test of the fit of any candidate expression for the spectral shape.

It should be noted that equation (2) has deliberately been chosen so that the curve passes beneath the points at high frequency ($x > 1.15$), because the points at short wavelength will include absorption by the so-called β-band (or *cis* band) of retinal (see e.g. Rodieck, 1973). Absorption in this subsidiary band becomes significant at a similar absolute wavelength (of about 450 nm) for pigments with different λ_{max}. Stavenga *et al.* (1993) have shown how this band can be fitted, but for the present purposes it was felt more appropriate to concentrate on the primary absorption band (the α-band), and for the time being to neglect the β-band.

The values of λ_{max} in Table 1 give the horizontal scaling needed to bring the raw results into alignment with the template curve of equation(2) in Figs 1 and 2. This fitting relied on sensitivity measurements primarily in the steeply declining long-wavelength part of the spectrum rather than in the region of the peak. Therefore the *separations* between the estimated values of λ_{max} should be quite reliable. On the other hand, the *absolute* values of the estimates of λ_{max} will depend on the accuracy of the template curve as a description of the peak of the spectrum. The shape of this curve near the peak was based primarily on the bovine rhodopsin absorbance measurements of Partridge and de Grip (1991) (★) in the linear plot of Fig. 2. Although equation (2) appears to provide a good description of those absorbance measurements, it remains possible that the λ_{max} values in Table 1 might be biased slightly from the true maxima.

The individual spectra

Up to this point the template curves have been compared with the experimental spectra on normalized abscissa scales. We now examine the fit of equation (2) to the individual spectra by re-plotting the symbols from Figs 1 and 2 against raw wavelength in Fig. 3. For convenience, the template curve of equation (2) is repeated here, in terms of λ and λ_{max}, as

$$S(\lambda) = \frac{1}{\{\exp a(A-\lambda_{max}/\lambda) + \exp b(B-\lambda_{max}/\lambda) + \exp c(C-\lambda_{max}/\lambda) + D\}} \quad (2')$$

When the raw results are plotted in this way, it can be seen that the template curve of equation (2′) provides a good fit to each individual set of points. The seven sets of solid symbols are from electrophysiological experiments on

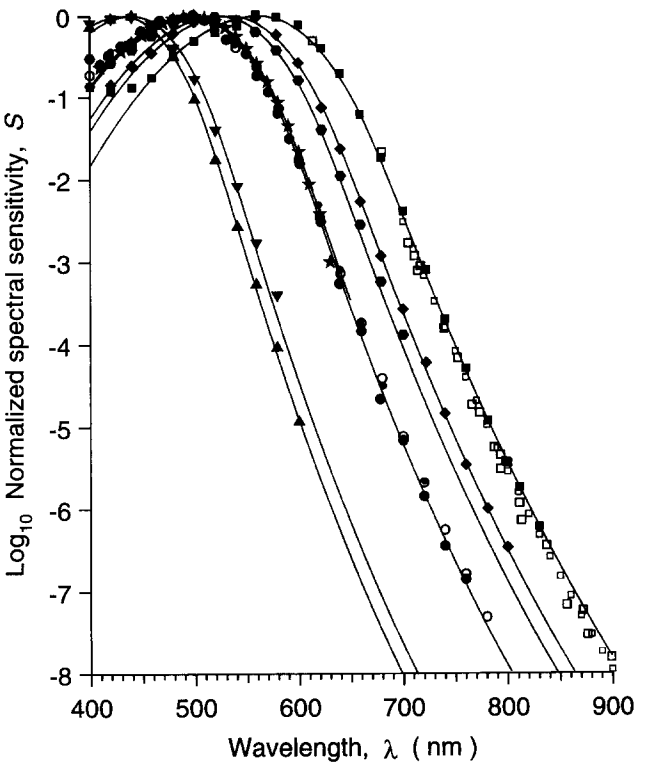

FIGURE 3. Individual measurements, as in the previous figures, replotted on a wavelength scale. The curves plot equation (2′), using the values of λ_{max} given against the respective symbols in Table 1; for the bovine absorbance measurements (★), the curve is only plotted to 650 nm.

photoreceptors (monkey cones, ■, ◆, ▲; squirrel cones, ●, ▼; monkey and human rods, ●, •), whereas the three sets of open symbols are from psychophysical experiments on human observers (photopic □, □; scotopic, ○). Note that, as explained in the Methods, these latter three sets of symbols have been converted to photon sensitivity terms, and corrected for self-screening and lens absorption.

In comparing the spectral sensitivities determined from psychophysical measurements with those obtained directly from electrophysiological recordings, it must be borne in mind that the precise positioning of the psychophysical curves will be influenced considerably by the parameter values chosen to correct for self-screening and pre-retinal filtering, as well as by the relative contribution of red and green cones to photopic sensitivity (see Methods). Uncertainties in these parameter values could readily lead to incorrect vertical positioning of the open symbols of 0.2 $\log_{10}$ units.

Nevertheless, the corrected spectral sensitivity for the scotopic visual system (○; from Crawford, 1949) is very similar to that obtained directly from isolated rod photoreceptors (●, •). Similarly, the corrected spectral sensitivities for photopic vision (□, □; from Goodeve, 1936; Griffin *et al.*, 1947) are reasonably close to the electrophysiological spectrum obtained in the 1980s from monkey red cones (■). There is, though, a suggestion that the points for photopic sensitivity might be shifted several nanometres to the left with respect to those for the red cone electrophysiology. However, the uncertainties

involved in conversion do not allow a firm conclusion to be drawn. Instead, a single template curve with $\lambda_{max} = 561$ nm has been plotted, and this provides a reasonable fit to the three sets of results. The similarity of the electrophysiological and corrected psychophysical sensitivity results would be consistent with the idea that, in the range 650–900 nm, human photopic sensitivity is determined exclusively by the responses of the red cones. [The spectral sensitivity of human red cones has been reported to be virtually identical to that of monkey red cones, but the values have not been tabulated (Schnapf *et al.*, 1987).]

The colour of light at long wavelengths

The ratio of red cone sensitivity to green cone sensitivity, R/G, determined from the measurements in Table 1 of Baylor *et al.* (1984), is plotted by the symbols in Fig. 4(A). At short wavelengths the red cones are less sensitive than the green cones, and the ratio becomes unity near 550 nm. At longer wavelengths the ratio progressively increases, until it reaches a maximum near 700 nm, after which it declines. The curve in Fig. 4(A) plots the theoretically expected ratio of red cone to green cone sensitivity, predicted by equation (2) using the values of λ_{max} given in Table 1; namely 561 nm for the red cones and 533 nm for the green cones. This curve, which exhibits a peak at 704 nm and equals unity at 546 nm, clearly provides a reasonable description of the measurements throughout the wavelength range from 500 to 800 nm.

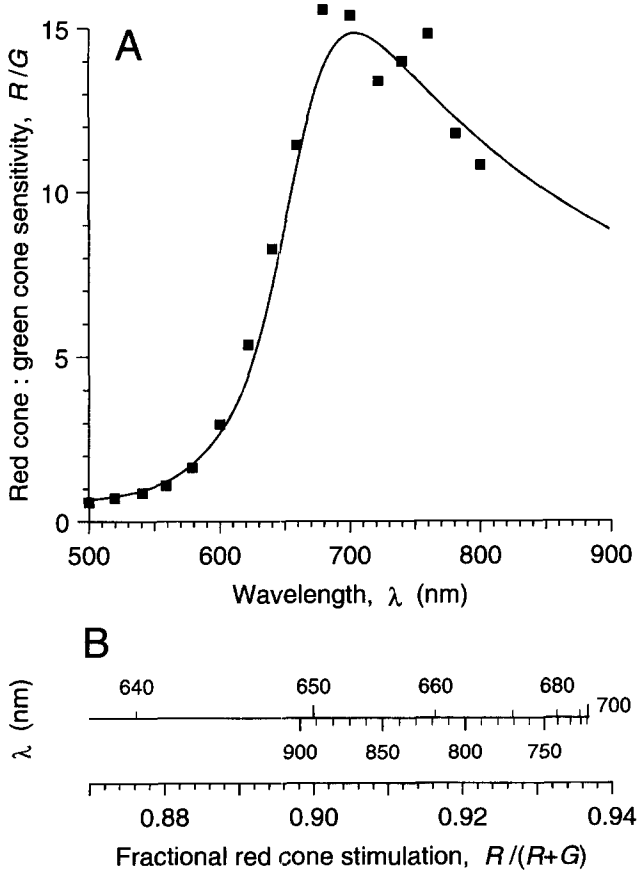

FIGURE 4. (A) Ratio of red cone to green cone sensitivity, R/G, as a function of wavelength. The symbols are from the electrophysiological recordings of Baylor *et al.* (1987, Table 1), with the minor correction mentioned in the Methods; and the curve is predicted by equation (2) with λ_{max} equal to 561 and 533 nm for the red and green cones respectively. (B) An alternative parametric plot of the predictions of equation (2). The fractional red cone stimulation, $R/(R + G)$, predicted by equation (2) with the above values of λ_{max}, is shown as a function of the wavelength of stimulation. As may be seen in (A), reversal occurs at a wavelength of about 704 nm. Pairs of wavelengths that elicit an equal R/G ratio in (A) lie opposite each other in (B).

For monkey, the sensitivity of the blue cones is at least a factor of 1000-fold below that of the green cones for all wavelengths beyond 560 nm (see Fig. 3, ▲ and ◆). For human receptors the peak of the blue cone sensitivity occurs at a wavelength even shorter than for monkey, at $\lambda_{max} \approx 420$ nm (see, e.g. Dartnall, Bowmaker & Mollon, 1983), while the red and green cone peaks are closely similar in the two species (Schnapf *et al.*, 1987). Hence it is reasonable to assume that human colour vision is essentially dichromatic at wavelengths greater than 550 nm, so that the colour of light at such wavelengths should be determined solely by the ratio of red cone to green cone sensitivity, i.e. by the ratio R/G plotted in Fig. 4(A). Any pair of wavelengths giving an equal ordinate value in Fig. 4(A) should be indistinguishable in colour, although it will of course be necessary to make the light at longer wavelength more intense in order for it to appear equally bright. Equation (2) therefore predicts that beyond about 704 nm the colour of light should revert from red towards orange, as was reported experimentally by Brindley (1955).

The theoretical curve in Fig. 4(A) has been replotted parametrically in Fig. 4(B), to show more clearly the predicted equivalence of different wavelengths. The abscissa in this panel represents the red cone signal as a fraction of the total signal; i.e. the ratio $R/(R + G)$. Even though electrophysiological measurements have not been made beyond 800 nm, it is nevertheless possible to examine the predicted equivalence out to longer wavelengths, since equation (2) is expected to apply asymptotically for small x (for long λ). The predicted equivalence of wavelengths in Fig. 4(B) is very similar to that found experimentally by Brindley (1955). In his experiments reversal occurred at around 700 nm, and a light of 850 nm was equivalent to one of 652 nm; according to the present analysis, reversal would be expected to occur at about 704 nm, and a light of 850 nm should be equivalent to one of 655 nm.

DISCUSSION

Common shape at long wavelengths

The present analysis extends Mansfield's (1985) finding of a common spectral shape for visual pigments to cover a much wider range. The scaling appears to hold not only near the peak, but also out to long wavelengths at which the sensitivity is down by as much as 9 $\log_{10}$ units. The closeness of the experimental points to a common curve has the consequence that the main absorption band (the α-band) of all the mammalian visual pigments examined can adequately be described by a single template. In view of the broadly similar variation of bandwidth as a

function of maximum frequency in other species (Ebrey & Honig, 1977), it seems reasonable to expect that this same template may also be applicable to retinal$_1$-based pigments in non-mammalian species as well.

Although the "tuning" of different visual pigments involves the substitution of amino acid residues at a number of separate sites (for review, see Nathans, Merbs, Sung, Weitz & Wang, 1992), the finding of a common template suggests that all these alterations act through a common physical mechanism. What seems to be important to photon absorption by the different visual pigments is simply the ratio of the photon's energy to some single constant: a characteristic energy of each visual pigment.

Goodeve (1936) found that at long wavelengths the human photopic sensitivity function declined exponentially as a function of frequency, so that a plot of log sensitivity against frequency asymptoted towards a constant slope. Stiles (1948) proposed a theoretical explanation for this behaviour, and predicted a limiting slope at long wavelengths of hc/kT ($=46.4$ $\log_e$ units μm per unit of reciprocal wavelength, at body temperature). He noted that the measured slope in the photopic system was 87% of this prediction, and that in the scotopic system it was 79% of the prediction. The present analysis extends these findings by showing that the normalized asymptotic slope appears to be invariant, with a value of 70 $\log_e$ units per unit of normalized frequency [see Fig. 1 and equation (2)]. Hence in different pigments the asymptotic slope is found to be directly proportional to the wavelength of maximal absorption; thus the asymptotic slope may be expressed as 70 $\log_e$ units $\times \lambda_{max}$.

In conjunction with Stiles' theory, this finding suggests the existence of a limiting value of λ_{max} for retinal$_1$-based visual pigments. This interpretation stems from the assumption that Stiles' prediction of hc/kT represents a theoretical maximum for the slope, i.e. that when account is taken of multiple vibrational modes, energy sub-states etc., the actual slope must be less than hc/kT. On this basis the limiting value of λ_{max} for retinal$_1$-based pigments is predicted to be $(hc/kT)/70$, or 663 nm. In fact the longest reported value of λ_{max} for a retinal$_1$-based pigment appears to be 575 nm for a frog cone (Liebman & Entine, 1968). The apparent absence of λ_{max} values between 575 nm and the predicted limit of 663 nm may arise from thermal instability in the pigment molecule. As the theoretical limit of λ_{max} were approached, it would seem likely that the visual pigment molecule might well exhibit an elevated rate of thermal isomerization, or some other kind of instability. Although such a pigment would exhibit good sensitivity at long wavelengths, this might be of no advantage to an organism if the pigment also exhibited excessive "dark light" (Barlow, 1957).

The template curve

The template curve, equation (2), provides the required asymptotic behaviour at long wavelengths, together with a good fit to the shape of the peak of the spectral curve. The dual requirement of accurately fitting the logarithmic plot of Fig. 1 (where sensitivity is followed to very long wavelengths) as well as the linear plot of Fig. 2 (where the absorbance measurements near the peak exhibit high accuracy) provides a stringent test of any candidate expression for spectral shape. Although equation (2) has no theoretical basis (apart from providing the required asymptotic decline at long wavelengths), it is a straightforward expression that is simple to evaluate numerically. Ideally one would wish to use an expression that was based on sound theoretical principles but, until a comprehensive physical theory is developed, this expression at least provides an accurate and relatively simple description of the results.

The equation presented here has significant advantages over the expressions given by Baylor *et al.* (1987) and Stavenga *et al.* (1993). The main drawback of the polynomial of Baylor *et al.* (1987) is that it exhibits the wrong behaviour at long wavelengths: after reaching a minimum of 10^{-7} at $\nu/\nu_{max} \approx 0.62$, it then rises rapidly and reaches unity at $\nu/\nu_{max} \approx 0.5$. The expression of Stavenga *et al.* (1993), on the other hand, has a discontinuity in slope, since their modified Gaussian expression is replaced by a constant slope below a criterion frequency.

Colour at long wavelengths

An important test of the accuracy of any expression for the spectral shape of visual pigments is its ability to predict the "yellowing" of colours that has been found to occur at long wavelengths for human observers with normal colour vision (Brindley, 1955). In Fig. 4(A) it is shown that equation (2) provides a good description of the measured ratio of red cone to green cone excitation in monkey photoreceptors (Baylor *et al.*, 1987), while comparison of the reversal in Fig. 4(B) with that found by Brindley indicates that the same expression provides an accurate description of the psychophysical phenomenon of yellowing. Hence equation (2) satisfies a third criterion for the form of the required spectral expression.

The position of the peak of the curve in Fig. 4(A), and the form of the reversal in Fig. 4(B), turn out not to be strongly dependent on the precise values of λ_{max} chosen for the red and green pigments (results not shown). The primary effect of altered λ_{max} values is to scale the height of the curve in Fig. 4(A). In order to obtain the illustrated close correspondence between the curve and the points it was necessary for the difference in λ_{max} between the red and green cones to be set close to 28 nm; each additional 1 nm difference led to an increase in the height of the peak of about 10%. It is for this reason that the λ_{max} for the green cones is obtained as 533 nm in the present paper, 2 nm greater than the value obtained by Baylor *et al.* (1987) from the same data.

REFERENCES

Barlow, H. B. (1957). Purkinje shift and retinal noise. *Nature*, *179*, 255–256.

Baylor, D. A., Nunn, B. J. & Schnapf, J. L. (1984). The photocurrent, noise and spectral sensitivity of rods of the monkey *Macaca fascicularis*. *Journal of Physiology*, *357*, 575–607.

Baylor, D. A., Nunn, B. J. & Schnapf, J. L. (1987). Spectral sensitivity of cones of the monkey *Macaca fascicularis*. *Journal of Physiology*, *390*, 145–160.

Brindley, G. S. (1955). The colour of light of very long wavelength. *Journal of Physiology*, *130*, 35–44.

Crawford, B. H. (1949). The scotopic visibility function. *Proceedings of the Physical Society, B*, *62*, 321–334.

Dartnall, H. J. A. (1953). The interpretation of spectral sensitivity curves. *British Medical Bulletin*, *9*, 24–30.

Dartnall, H. J. A. (1968). The photosensitivities of visual pigments in the presence of hydroxylamine. *Vision Research*, *8*, 339–358.

Dartnall, H. J. A. & Goodeve, C. F. (1937). Scotopic luminosity curve and the absorption spectrum of visual purple. *Nature*, *139*, 409–411.

Dartnall, H. J. A., Bowmaker, J. K. & Mollon, J. D. (1983). Human visual pigments: Microspectrophotometric results from the eyes of seven persons. *Proceedings of the Royal Society of London B*, *220*, 115–130.

Ebrey, T. G. & Honig, B. (1977). New wavelength dependent visual pigment nomograms. *Vision Research*, *17*, 147–151.

Goodeve, C. F. (1936). Relative luminosity in the extreme red. *Proceedings of the Royal Society, A*, *155*, 664–683.

Griffin, D. R., Hubbard, R. & Wald, G. (1947). The sensitivity of the human eye to infra-red radiation. *Journal of the Optical Society of America*, *37*, 546–554.

Kraft, T. W. (1988). Photocurrents of cone photoreceptors of the golden-mantled ground squirrel. *Journal of Physiology*, *404*, 199–213.

Kraft, T. W., Schneeweis, D. M. & Schnapf, J. L. (1993). Visual transduction in human rod photoreceptors. *Journal of Physiology*, *464*, 77–765.

Lewis, P. R. (1955). A theoretical interpretation of spectral sensitivity curves at long wavelengths. *Journal of Physiology*, *130*, 45–52.

Liebman, P. A. & Entine, G. (1968). Visual pigments of frog and tadpole. *Vision Research*, *8*, 761–775.

Mansfield, R. J. W. (1985). Primate photopigments and cone mechanisms. In Fein, A. & Levine, J. S. (Eds), *The visual system* (pp. 89–106). New York: Alan Liss.

Mansfield, R. J. W., Levine, J. S., Lipetz, L. E., Collins, B. A, Raymond, G. & MacNichol, E. F. (1984). Blue sensitive cones in the primate retina: Microspectrophotometry of the visual pigment. *Brain Research*, *56*, 389–394.

Mollon, J. D. & Bowmaker, J. K. (1992). The spatial arrangement of cones in the primate fovea. *Nature*, *360*, 677–692.

Nathans, J., Merbs, S. L., Sung, C.-H., Weitz, C. J. & Wang, Y. (1992). Molecular genetics of human visual pigments. *Annual Review of Genetics*, *26*, 403–424.

Partridge, J. C. & de Grip, W. J. (1991). A new template for rhodopsin (vitamin A_1 based) visual pigments. *Vision Research*, *31*, 619–630.

Pinegin, N. I. (1945). Absolute sensitivity of the eye in infra-red spectrum. *Comptes Rendus (Doklady) de l'Academie des Sciences de l'URSS*, *67*, 627–629.

Rodieck, R. W. (1973). *The vertebrate retina. Principles of structure and function*. San Francisco, Calif.: W.H. Freeman.

Schnapf, J. L., Kraft, T. W. & Baylor, D. A. (1987). Spectral sensitivity of human cone photoreceptors. *Nature*, *325*, 439–441.

Stavenga, D. G., Smits, R. P. & Hoenders, B. J. (1993). Simple exponential functions describing the absorbance bands of visual pigment spectra. *Vision Research*, *33*, 1011–1017.

Stiles, W. S. (1948). The physical interpretation of the spectral sensitivity curve of the eye. In *Transactions of the optical convention of the Worshipful Company of Spectacle Makers* (pp. 97–107). London: Spectacle Makers' Co. [Reprinted in Stiles, W. S. (1978). *Mechanisms of colour vision*. London: Academic Press.]

Stockman, A., MacLeod, D. I. A. & Johnson, N. E. (1993). Spectral sensitivities of the human cones. *Journal of the Optical Society of America*, *10*, 2491–2521.

Wald, G. (1945). Human vision and the spectrum. *Science*, *101*, 653–658.

Walraven, P. L. (1974). A closer look at the tritanopic convergence point. *Vision Research*, *14*, 1339–1343.

Wyszecki, G. & Stiles, W. S. (1982). *Color science. Concepts and methods, quantitative data and formulas*. New York: Wiley.

Acknowledgements—I wish to thank Drs Bob Rodieck and Pieter Walraven for helpful comments on the manuscript. Supported by grants from the Wellcome Trust (034792), the European Commission (SSS 6961) and the Human Frontiers Science Program (RG-62/94).